PHYSICAL REVIEW B VOLUME 16, NUMBER 4 15 AUGUST 1977

Unified computation scheme of low-energy electron diffraction—the combined-space method*

S. Y. Tong and M. A. Van Hove†
Department of Physics and Surface Studies Laboratory, University of Wisconsin-Milwaukee, Milwaukee, Wisconsin 53201
(Received 3 January 1977)

A new microscopic method for the evaluation of reflected elastic intensities of low-energy electron diffraction from crystal surfaces is developed. This method divides layers of a crystal into subgroups. Layers having small interlayer separations with their neighbors form a subgroup and are solved in the L-space representation using iterations, matrix inversions, or a combination of both. Results of each subgroup are transformed to the K-space representation. Multiple scattering between subgroups and other crystal layers separated by larger interlayer spacings are solved in K space. The scheme is particularly useful in analyzing surface structures where coplanar or near coplanar layers are mixed together with other layers having larger separation distances. Some examples of these are the chemisorption of hydrogen and small gas atoms on open crystal faces, the surface structures of reconstructed and unreconstructed semiconductors and layer compounds, and the reconstructed faces of some transition metals, etc.

I. INTRODUCTION

The theoretical treatment of low-energy electron diffraction from clean and chemisorbed crystal layers sprouted a number of powerful microscopic methods in the past few years.[1,2] Among them, Beeby[3] formulated a T-matrix inversion method based on evaluating and solving a system of layer-scattering matrices expressed in the L (angular momentum) space representation. A parallel treatment was developed by McRae,[4,5] who expressed the propagation and scattering of an electron between layers in K (linear momentum) space. This second method was put into efficient use by Jepsen, Marcus, and Jona,[6,7] who called their version the layer-KKR (Korringa-Kohn-Rostoker) method. Both the L-space and K-space methods have been used to calculate intensity-voltage curves of a number of clean and overlayer systems, and good agreement with experiment was obtained. Since these two methods include interatomic scattering events to all orders by exactly solving systems of matrix equations, they do not take advantage of the fact that an electron in the 20–400-eV range has only a short mean free path. Within this short path length (4–12 Å), only the first few interatomic scattering events can be important.

Recognition of this fact leads to the development of a number of "fast" methods.[8-16] The fast methods are based on including only a subset of interatomic scattering events. If all important scattering events are included in this subset, the resulting method is computationally efficient and numerically accurate. Two most successful fast methods are the renormalized-forward-scattering (RFS) method[12,13] and the layer-doubling method,[14-16] originally developed by Pendry. Both methods start out with the exact layer-scattering matrix in the K-space representation. In the RFS scheme, forward interlayer scattering events are iteratively accumulated and back interlayer scattering events are summed sequentially. The summation over successive orders of back scattering events is stopped if numerical convergence to a desired accuracy is reached. Thus, wherever there is convergence of the power-series expansion of back scattering matrices, the RFS method is fast and can be rapidly carried to a high degree of numerical accuracy. The layer-doubling method, on the other hand, includes a larger set of scattering events than RFS. It generates the exact solutions of forward and back layer-scattering matrices in the K-space representation for two layers. The procedure is then repeated to generate the scattering matrices for four, eight, etc., layers. This process converges in typically three to four iterations.

II. NEED FOR FURTHER FAST COMPUTATION SCHEMES

The RFS and layer-doubling methods have been applied to the determination of surface structures of clean and overlayer systems. They were fast and produced numerically accurate results for a large number of materials and crystal structures.[16-19] However, there are important groups of materials and overlayer systems whose surface structures are not suitable for the application of these methods. Some examples are the chemisorption of gas atoms (e.g., C, N, or O) on open faces of metals and semiconductors, the adsorption of hydrogen on all crystal faces, transition metals with reconstructed layers, reconstructed and unreconstructed faces of semiconductors, and layer compounds. This is because RFS and layer doubling, as well as the layer-KKR exact method, de-

scribe interlayer scattering by matrices $M^{\pm\pm}_{\vec{g}\vec{g}}$, whose dimension is g, the number of plane-wave components. At small interlayer distances, the number g can get very big. The number of plane-wave components g increases roughly as d^{-2}, where d is the interlayer separation. An estimate of the number of plane waves which must be included is given in the Appendix. It is equal to

$$g \simeq AE/2\pi + (A/4\pi)(\ln t/d)^2 , \tag{1}$$

where E is the energy (in hartrees, i.e., double rydbergs), A is the unit-cell area (in square Bohr radii), d is the interlayer spacing (in Bohr radii), and t is the desired fractional decay of exponential waves over the interlayer spacing d. Thus the dimension of $M^{\pm\pm}_{\vec{g}'\vec{g}}$ increases rapidly as d gets small [e.g., for $d \approx 0.3$ Å, at $E = 100$ eV and $t = 0.002$, $g \gtrsim 200$ in 1×1 structures and $g \gtrsim 800$ in 2×2 structures]. Overtruncation of the number of g to manageable dimensions of $M^{\pm\pm}_{\vec{g}'\vec{g}}$ often leads to numerically unstable results. It is estimated that under normal conditions, RFS becomes numerically unreliable at about $d \leq 0.9$ Å, the layer-KKR and layer-doubling methods at about $d \leq 0.5$ Å. It is true that such numerical instability may be avoided by the use of a bigger computer with more core space (thus allowing the dimension of $M^{\pm\pm}_{\vec{g}'\vec{g}}$ to increase) and better accuracy (so it can handle accurately large-sized matrix operations). However, when g gets big ($g \geq 200$), methods based on the K-space representation become increasingly cumbersome and numerically unreliable.

III. L-SPACE ITERATION SCHEME

An obvious solution of treating crystal structures with near coplanar layers is to go back to the angular momentum representation. In the L-space representation, the layer-scattering matrices have dimensions independent of g. This is because an explicit sum over plane waves is carried out. The resulting scattering matrices have dimension $L = \bar{N}^2$, where $\bar{N}$ is the number of phase shifts necessary for proper representation of the atomic scattering. On the other hand, it is usually more convenient to express electron propagation between layers in terms of plane waves, because this choice leads to diagonal interlayer propagation matrices $R^{\pm}_{\vec{g}}\delta_{\vec{g}\vec{g}'}$; however, the use of plane waves requires good convergence of the plane-wave expansion. Such convergence is difficult to achieve where the interlayer spacing is small.

The T-matrix inversion method of Beeby[3] is an L-space method, where multiple-scattering events among a finite number of atomic layers are included to all scattering orders. However, while this method is conceptually sound, its computation procedure is not suitable for an actual structure determination. This is because a final matrix equation solution, the most time-consuming step of the procedure, involving all atomic layers of the crystal, must be carried out repeatedly for *each* trial structure. Zimmer and Holland[20] proposed a faster scheme based on iterations of Beeby's formulas. They named this scheme the reverse-scattering-perturbation method, which we shall briefly describe here.

Starting with Beeby's formula, if we define layer scattering vectors

$$T_{iL}(\vec{k}^{+}(\vec{0})) = \sum_{L'} T^{i}_{LL'}(\vec{k}^{+}(\vec{0}))Y^{*}_{L'}(\vec{k}^{+}(\vec{0})) \tag{2}$$

and

$$\tau_{iL}(\vec{k}^{+}(\vec{0})) = \sum_{L'} \tau^{i}_{LL'}(\vec{k}^{+}(\vec{0}))Y^{*}_{L'}(\vec{k}^{+}(\vec{0})) , \tag{3}$$

then the final reflected amplitude may be written[1]

$$T(\vec{k}^{-}(\vec{g}),(\vec{k}^{+}(\vec{0})) = \gamma_0 \sum_{L} \frac{Y_L(\vec{k}^{-}(\vec{g}))}{k^{+}_{i}(\vec{g})} \sum_{i} \left[e^{i[\vec{k}^{+}(\vec{0})-\vec{k}^{-}(\vec{g})]\cdot\vec{d}_i} T_{iL}(\vec{k}^{+}(\vec{0}))\right] , \tag{4}$$

where i is the atomic plane index, $\vec{k}^{+}(\vec{0})$ and $\vec{k}^{-}(\vec{g})$ are the incident and reflected directions, respectively, and $\gamma_0 = -(8\pi^2 i/A)(2m/\hbar^2)F(k_0)$. Usually, $F(k_0)$ is set equal to unity. The electron amplitude at the ith plane is expressed in the vector $T_{iL}(\vec{k}^{+}(\vec{0}))$ obtained from[2]

$$T_{iL}(\vec{k}^{+}(\vec{0})) = \tau_{iL}(\vec{k}^{+}(\vec{0})) + \sum_{n=0}^{M} [T^{+(n)}_{iL}(\vec{k}^{+}(\vec{0})) + T^{-(n)}_{iL}(\vec{k}^{+}(\vec{0}))] . \tag{5}$$

In Eq. (5), $T^{\pm(n)}_{iL}(\vec{k}^{+}(\vec{0}))$ are results of electron amplitudes at plane i after n iterations. The lowest order ($n = 0$) contains at least two scattering events, i.e., 2nd order in $\tau^{i}_{LL'}(\vec{k}^{+}(\vec{0}))$. The (−) sign is for scattering into deeper layers, the (+) sign for outward scattering, with index n denoting the number of times the electron path has changed directions, i.e., from (+) to (−) or vice versa (n is also the iteration order). The iteration relations are[2,20]

$$T^{+(n)}_{iL}(\vec{k}^{+}(\vec{0})) = \sum_{L_1L_2} \tau^{i}_{LL_1}(\vec{k}^{+}(\vec{0})) \sum_{j>i} G^{ij}_{L_1L_2}(\vec{k}^{+}(\vec{0})) \times [T^{+(n)}_{jL_2}(\vec{k}^{+}(\vec{0})) + T^{-(n-1)}_{jL_2}(\vec{k}^{+}(\vec{0}))] \tag{6}$$

and

$$T_{iL}^{-(n)}(\vec{k}^+(\vec{0})) = \sum_{L_1 L_2} \tau_{LL_1}^{i}(\vec{k}^+(\vec{0})) \sum_{j<i} G_{L_1 L_2}^{ij}(\vec{k}^+(\vec{0})) \times [T_{jL_2}^{-(n)}(\vec{k}^+(\vec{0})) + T_{jL_2}^{+(n-1)}(\vec{k}^+(\vec{0}))] . \quad (7)$$

The initial conditions are[2,20]

$$T_{1L}^{-(n)}(\vec{k}^+(\vec{0})) = 0, \quad n = 0, 1, 2 \ldots , \quad (8)$$

$$T_{NL}^{+(n)}(\vec{k}^+(\vec{0})) = 0, \quad n = 0, 1, 2 \ldots , \quad (9)$$

because no electron amplitude can be scattered from above the top layer ($i = 1$) or below the deepest layer ($i = N$). Also, we must put the starting conditions as

$$T_{iL}^{-(-1)}(\vec{k}^+(\vec{0})) = \tau_{iL}(\vec{k}^+(\vec{0})), \quad i = 2, 3, \ldots , N , \quad (10)$$

$$T_{iL}^{+(-1)}(\vec{k}^+(\vec{0})) = \tau_{iL}(\vec{k}^+(\vec{0})), \quad i = 1, 2, \ldots , N-1 , \quad (11)$$

and

$$T_{1L}^{-(-1)}(\vec{k}^+(\vec{0})) = T_{NL}^{+(-1)}(\vec{k}^+(\vec{0})) = 0 .$$

This is because the incident electron can propagate to any layer i with no scattering and one must include the initial scattering $\tau_{iL}(\vec{k}^+(\vec{0}))$ at the ith layer.

The sum over iteration order n in Eq. (5) is carried until numerical convergence is achieved. Usually, this occurs at about five iterations. Evaluation of the vectors $T_{iL}^{\pm(n)}(\vec{k}^+(\vec{0}))$ in Eqs. (6) and (7) involves first generating interlayer structure propagators $G_{LL'}^{ij}(\vec{k}^+(\vec{0}))$ defined by Beeby.[3]

The method of Zimmer and Holland[20] contains no matrix of dimension g. The layer vectors $T_{iL}^{\pm}(\vec{k}^+(\vec{0}))$ and matrices $G_{LL'}^{ij}(\vec{k}^+(\vec{0}))$ have dimension L. For almost all practical materials, nine phase shifts in the energy range 0–300 eV seem to do an adequate job. Thus, this L-space iteration method has a clear advantage in speed and numerical reliability over K-space methods (e.g., RFS, layer doubling, layer KKR) when the number of beams gets much larger than 81.

However, there is an undesirable feature of this method which restricts its being generally used in structure analysis. The method calls for the evaluation and storage of interlayer propagation matrices $G_{LL'}^{ij}(\vec{k}^+(\vec{0}))$ which are square matrices. There are a total of $N(N-1)$ such matrices for N layers of a lattice. For varying the interlayer spacings of three surface layers of a 10-layer crystal, 48 $L \times L$ square matrices must be recalculated at each new geometry. Clearly, this method is computationally unattractive when such large numbers of $G_{LL'}^{ij}(\vec{k}^+(\vec{0}))$ must be recalculated at each structure.

IV. COMBINED SPACE METHOD

From the foregoing discussions, it is clear that in the K-space representation, the main advantage is that interlayer propagators $R_{\vec{g}}^{\pm}\delta_{\vec{g}\vec{g}'}$ are diagonal in form and only depend on $\vec{d} = \vec{d}_{i+1} - \vec{d}_i$, the interlayer vector between successive layers. Another attractive feature is that symmetry of the lattice can be exploited rather easily to cut down computation time and core storage. The L-space representation avoids matrices with dimension g, the price to pay is dealing with square matrices $G_{LL'}^{ij}(\vec{k}^+(\vec{0}))$ which depend on distances $\vec{d}_i - \vec{d}_j$ between *each pair* of layers. In systems of practical importance, such as the chemisorption of small gas atoms or the rearrangement of some semiconductor and transition metal surfaces, it is generally true that only a few (two or three) surface layers are closely spaced or coplanar, while deeper layers remain at larger, bulk spacings. To treat the entire crystal with an L-space method would involve evaluating the many $G_{LL'}^{ij}(\vec{k}^+(\vec{0}))$ matrices. Similarly, RFS, layer-doubling, or the layer-KKR method would be inadequate because of the large number of beams associated with the small surface spacings. The best solution is a method which combines the strong features of each representation and applies each representation to the regime it is best suited for, L space for small d spacings (<1.0 Å) and K space for larger, bulklike spacings (≥1.0 Å). We shall call such a formulation the combined space method and present it in the following.

First, we define vectors for incident beams $\vec{k}^{\pm}(\vec{g})$ from above [the (+) sign] and below [the (–) sign] on the ith layer

$$T_{iL}(\vec{k}^{\pm}(\vec{g})) = \sum_{L'} T_{LL'}^{i}(\vec{k}^{\pm}(\vec{g})) Y_{L'}^{*}(\vec{k}^{\pm}(\vec{g})) \quad (12)$$

and

$$\tau_{iL}(\vec{k}^{\pm}(\vec{g})) = \sum_{L'} \tau_{LL'}^{i}(\vec{k}^{\pm}(\vec{0})) Y_{L'}^{*}(\vec{k}^{\pm}(\vec{g})) . \quad (13)$$

Then the interlayer matrices $G_{LL'}^{ij}(\vec{k}^{\pm}(\vec{g}))$ are defined for general incident directions

$$G_{LL'}^{ij}(\vec{k}^{\pm}(\vec{g})) = e^{-i\vec{k}^{\pm}(\vec{g})\cdot(\vec{d}_i - \vec{d}_j)} \hat{G}_{LL'}^{ij}(\vec{k}^+(\vec{0})), \quad (14)$$

where[1]

$$\hat{G}_{LL'}^{ij}(\vec{k}^+(\vec{0})) = \sum_{\vec{P}} \sum_{L_1} \lambda k_0 i^{l_1} a(LL'L_1) h_{l_1}^{(1)}(k_0 | \vec{P} + \vec{d}_i - \vec{d}_j |) \times Y_L(\vec{P} + \vec{d}_i - \vec{d}_j) e^{-i\vec{k}^+(\vec{0})\cdot\vec{P}} , \quad (15)$$

$$\hat{G}^{ij}_{LL'}(\vec{k}^{+}(\vec{0})) = \gamma_0 \sum_{\vec{g}_1} \frac{e^{i\vec{k}^{\pm}(\vec{g}_1)\cdot(\vec{d}_i-\vec{d}_j)}}{k_\perp^{+}(\vec{g}_1)} \times Y^{*}_{L}(\vec{k}^{\pm}(\vec{g}_1)) Y_{L'}(\vec{k}^{\pm}(\vec{g}_1)). \quad (16)$$

In Eq. (15), $\lambda = -4\pi i(2m/\hbar^2)F(k_0)$, $F(k_0)=1$, and $h_l^{(1)}(x)$ is the spherical Hankel function. In Eq. (16), the (+) sign in the sum over $\vec{g}_1$ is for $(\vec{d}_i-\vec{d}_j)_\perp > 0$ and the (−) sign for $(\vec{d}_i-\vec{d}_j)_\perp < 0$. Within closely spaced layers i and j, the number of required beams g_1 is large [e.g., over 200 beams for $(\vec{d}_i-\vec{d}_j)_\perp \approx 0.3$ Å]. But the matrices $G^{ij}_{LL'}(\vec{k}^{\pm}(\vec{g}))$ have dimension L, independent of the number $\vec{g}_1$. The sum over real space in Eq. (15) is valid whether $(\vec{d}_i-\vec{d}_j)_\perp = 0$ or not, and this sum can be advantageously used in cases where the summation over $\vec{g}_1$ in Eq. (16) [which is valid only for $(\vec{d}_i-\vec{d}_j)_\perp \neq 0$] requires an excessive number of beams.

The layer vectors $T_{iL}(\vec{k}^{\pm}(\vec{g}))$ are first solved for the closely spaced layers (say $i=1, 2, 3$, etc.) using, for example, the L-space iteration method given in Eqs. (5)–(11), properly extended for general incident directions $\vec{k}^{\pm}(\vec{g})$. Then transmission and reflection matrices are formed in K space for the group (or groups) of closely spaced layers. For illustration, let us take a specific example of two closely spaced layers (i and $i+1$), shown in Fig. 1. In the figure, we have chosen $i=1$. We define propagation vectors

$$R(\vec{g}^{+}) = e^{i\vec{k}^{+}(\vec{g})\cdot\vec{d}_s}, \quad (17)$$

$$R(\vec{g}^{-}) = e^{-i\vec{k}^{-}(\vec{g})\cdot\vec{d}_s}, \quad (18)$$

where[1]

$$\vec{k}^{\pm}(\vec{g}) = (\vec{k}_{i\parallel}+\vec{g}; \pm[(2m/\hbar^2)[E-\Sigma(E)] - (\vec{k}_{i\parallel}+\vec{g})^2]^{1/2}\vec{e}_\perp), \quad (19)$$

$\vec{d}_s$ is the surface interlayer spacing, and $\vec{e}_\perp$ a unit vector pointing inwards normal to the surface. The transmission and reflection matrices for the two-layer composite are

$$(M^{++}_{i,i+1})_{\vec{g}'\vec{g}} = \gamma_0 \sum_L \frac{Y_L(\vec{k}^{+}(\vec{g}'))}{k_\perp^{+}(\vec{g}')}[R(\vec{g}'^{+})T_{iL}(\vec{k}^{+}(\vec{g})) + T_{i+1,L}(\vec{k}^{+}(\vec{g}))R(\vec{g}^{+})], \quad (20)$$

$$(M^{-+}_{i,i+1})_{\vec{g}'\vec{g}} = \gamma_0 \sum_L \frac{Y_L(\vec{k}^{-}(\vec{g}'))}{k_\perp^{+}(\vec{g}')}[T_{iL}(\vec{k}^{+}(\vec{g})) + R(\vec{g}'^{-}) \times T_{i+1,L}(\vec{k}^{+}(\vec{g}))R(\vec{g}^{+})] \quad (21)$$

for beams $\vec{k}^{+}(\vec{g})$ incident from above, and

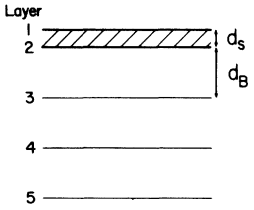

FIG. 1. Schematic diagram of two surface layers, separated by interlayer spacing d_s and bulk layers, separated by d_B.

$$(M^{--}_{i,i+1})_{\vec{g}'\vec{g}} = \gamma_0 \sum_L \frac{Y_L(\vec{k}^{-}(\vec{g}'))}{k_\perp^{+}(\vec{g}')}[T_{iL}(\vec{k}^{-}(\vec{g}))R(\vec{g}^{-}) + R(\vec{g}'^{-})T_{i+1,L}(\vec{k}^{-}(\vec{g}))], \quad (22)$$

$$(M^{+-}_{i,i+1})_{\vec{g}'\vec{g}} = \gamma_0 \sum_L \frac{Y_L(\vec{k}^{+}(\vec{g}'))}{k_\perp^{+}(\vec{g}')}[R(\vec{g}'^{+})T_{iL}(\vec{k}^{-}(\vec{g})) \times R(\vec{g}^{-}) + T_{i+1,L}(\vec{k}^{-}(\vec{g}))] \quad (23)$$

for beams $\vec{k}^{-}(\vec{g})$ incident from below. It is important to note that $\vec{g}$ corresponds to the beam set of the larger d spacing of the solid (d_B in Fig. 1). The number g is substantially smaller than g_1, the latter being the number of beams for the closely spaced surface layers (typically, for 1×1 structures, $g \approx 21$ and $g_1 \gtrsim 200$ for $d_s \approx 0.3$ Å and $d_B \approx 1.7$ Å). The transmission and reflection matrices [Eqs. (20)–(23)] defined for the set of closely spaced layers are then used to solve for the reflectivity of the crystal using any one of the established K-space schemes (e.g., RFS, layer-doubling, or layer-KKR method, etc.). Although Eqs. (20)–(23) are written explicitly for the case of two layers (i and $i+1$), their extension to three or more closely spaced layers is straightforward, involving essentially kinematiclike relations between the set of layer vectors $T_{iL}(\vec{k}^{\pm}(\vec{g}))$.

V. COMBINED SPACE METHOD WITH MATRIX INVERSION

The L-space iterations for a set of closely spaced layers i, j, k, etc., essentially group power-series expansions with terms of the form

$$\underline{\tau}^{i}(\vec{k}^{+}(\vec{0}))\underline{G}^{ij}(\vec{k}^{\pm}(\vec{g}))\underline{\tau}^{j}(\vec{k}^{+}(\vec{0})) \times \underline{G}^{jk}(\vec{k}^{\pm}(\vec{g}))\underline{\tau}^{k}(\vec{k}^{+}(0))Y^{*}(\vec{k}^{\pm}(\vec{g})), \quad (24)$$

where

$$\underline{\tau}^{i}(\vec{k}^{+}(\vec{0})) = \underline{t}_i[\underline{1} - \underline{G}^{sp}(\vec{k}^{+}(\vec{0}))\underline{t}_i]^{-1} \quad (25)$$

is the usual planar scattering matrix defined in the L-space representation.[1] Insomuch as the power-series expansion in $\underline{\tau}^{i}(\vec{k}^{+}(\vec{0}))$ and $\underline{G}^{ij}(\vec{k}^{\pm}(\vec{g}))$ converges, the iteration procedure is applicable for all interlayer distances, including coplanar layers. However, it is possible that the expansion could

diverge for, say, a pair of strong scattering layers i and j, coplanar or otherwise. In other words, an expansion like

$$\underline{\tau}^{i}(\vec{k}^{+}(\vec{0}))\underline{G}^{ij}(\vec{k}^{\pm}(\vec{g}))\underline{\tau}^{j}(\vec{k}^{+}(\vec{0})) \times \underline{G}^{ji}(\vec{k}^{\pm}(\vec{g}))\underline{\tau}^{i}(\vec{k}^{+}(\vec{0}))Y^{*}(\vec{k}^{\pm}(\vec{g}))+\cdots, \quad (26)$$

etc., diverges. Wherever this happens, a new procedure must be used to properly treat multiple scatterings between layers i and j. Such a treatment is given below.

It should be noted that failures of expansions like Eq. (26) to converge upon iteration, or similar failures where RFS diverges upon iteration, do not mean the basic premise, that a low-energy electron has a short mean free path, becomes invalid for scatterings in layers i and j. It only means that the particular way of packaging, that of grouping scattering events between atoms into layer-scattering matrices $\tau^{i}_{LL'}(\vec{k}^{+}(\vec{0}))$ (or $M^{\pm\pm}_{\vec{g}\vec{g}'}$ in RFS), and then expanding them in a power series, would no longer produce numerical results representative of the actual physical process. The physical process of a low-energy electron scattering among atoms always has a short mean free path (except near the Fermi level where there is no inelastic damping). It is rather the numerical packaging that sometimes fails. When this numerical failure occurs, a different computation procedure must be sought.

Let us envision the following surface structure (Fig. 2). Layers 1–4 are closely spaced and should be treated in L space. Of these, layers 2 and 3 are strong scatterers and have a particularly small interlayer separation. Let us assume they cannot be summed by L-space iteration and must be treated by another method. Layers 5–N have the larger bulk-type spacings (e.g., $d_B \approx 1.7$ Å). The procedure is as follows: Scattering events between layers 2 and 3 are first summed to form subgroup A. Then layer 1, subgroup A, and layer 4 are summed by L-space iterations to form subgroup B. Finally, subgroup B, layers 5–N are treated in K space to obtain reflected intensities. In Fig. 2, the layers are shown as noncoplanar. However, the formulas given below are general and may be applied to different combinations of coplanar and noncoplanar layers in each subgroup. Also, the numbers of layers in subgroups A and B are arbitrary, not necessarily restricted to 2 and 4, as given in this example.

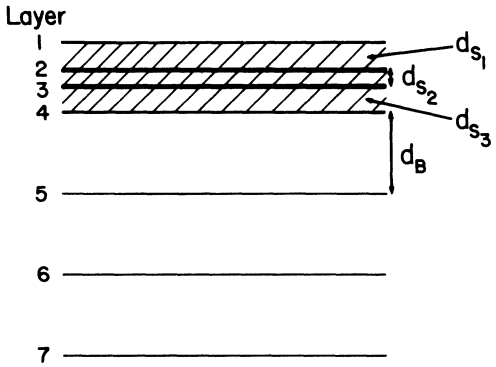

FIG. 2. Schematic diagram of four surface layers, with interlayer separations d_{s1}, d_{s2}, d_{s3} and bulk layers with separation d_B.

Multiple scattering events in layers 2 and 3 are first treated by matrix inversion. To do this, we form matrices $\overline{T}^{ij}_{LL'}(\vec{k}^{\pm}(\vec{g}))$ for $i,j=2,3$ by

$$\overline{T}^{ij}_{LL'}(\vec{k}^{\pm}(\vec{g}))=\tau^{i}_{LL'}(\vec{k}^{+}(\vec{0}))\delta_{ij}+\sum_{q\neq i}\tau^{i}_{LL_1}(\vec{k}^{+}(\vec{0})) \times G^{iq}_{L_1L_2}(\vec{k}^{\pm}(\vec{g}))\overline{T}^{qj}_{L_2L'}(\vec{k}^{\pm}(\vec{g})), \quad q=2 \text{ or } 3. \quad (27)$$

Explicitly, $\underline{\overline{T}}^{ij}(\vec{k}^{\pm}(\vec{g}))$ have the following form ($i=2$ in this example):

$$\begin{pmatrix} \underline{\overline{T}}^{ii}(\vec{k}^{\pm}(\vec{g})) & \underline{\overline{T}}^{i,i+1}(\vec{k}^{\pm}(\vec{g})) \\ \underline{\overline{T}}^{i+1,i}(\vec{k}^{\pm}(\vec{g})) & \underline{\overline{T}}^{i+1,i+1}(\vec{k}^{\pm}(\vec{g})) \end{pmatrix} = \begin{pmatrix} 1 & -\underline{\tau}^{i}(\vec{k}^{+}(\vec{0}))\underline{G}^{i,i+1}(\vec{k}^{\pm}(\vec{g})) \\ -\underline{\tau}^{i+1}(\vec{k}^{+}(\vec{0}))\underline{G}^{i+1,i}(\vec{k}^{\pm}(\vec{g})) & 1 \end{pmatrix}^{-1} \begin{pmatrix} \underline{\tau}^{i}(\vec{k}^{+}(0)) & 0 \\ 0 & \underline{\tau}^{i+1}(\vec{k}^{+}(\vec{0})) \end{pmatrix}. \quad (28)$$

At first glance, solution of Eq. (28) seems to require $2g$ matrix inversions, due to the dependence of $\underline{G}^{ij}(\vec{k}^{\pm}(\vec{g}))$ on $\vec{k}^{\pm}(\vec{g})$. One can avoid this dilemma by noticing in Eq. (14) that $\underline{G}^{ij}(\vec{k}^{\pm}(\vec{g}))$ may be written

$$G^{ij}_{LL'}(\vec{k}^{+}(\vec{g}))=[R^{i}(\vec{g}^{+})]^{-1}R^{j}(\vec{g}^{+})\hat{G}^{ij}_{LL'}(\vec{k}^{+}(\vec{0})) \quad (29)$$

and

$$G^{ij}_{LL'}(\vec{k}^{-}(\vec{g}))=R^{i}(\vec{g}^{-})[R^{j}(\vec{g}^{-})]^{-1}\hat{G}^{ij}_{LL'}(\vec{k}^{+}(\vec{0})). \quad (30)$$

The $\vec{k}^{\pm}(\vec{g})$ dependence in Eq. (28) then factors out as

$$\begin{pmatrix} \underline{T}^{i,i}(\vec{k}^+(\vec{g})) & \underline{T}^{i,i+1}(\vec{k}^+(\vec{g})) \\ \underline{T}^{i+1,i}(\vec{k}^+(\vec{g})) & \underline{T}^{i+1,i+1}(\vec{k}^+(\vec{g})) \end{pmatrix} = \begin{pmatrix} R^i(\vec{g}^+)\underline{1} & 0 \\ 0 & R^{i+1}(\vec{g}^+)\underline{1} \end{pmatrix}^{-1} \begin{pmatrix} \underline{1} & -\underline{\tau}^i(\vec{k}^+(\vec{0}))\underline{\hat{G}}^{i,i+1}(\vec{k}^+(\vec{0})) \\ -\underline{\tau}^{i+1}(\vec{k}^+(\vec{0}))\underline{\hat{G}}^{i+1,i}(\vec{k}^+(\vec{0})) & \underline{1} \end{pmatrix}^{-1}$$
$$\times \begin{pmatrix} \underline{\tau}^i(\vec{k}^+(\vec{0})) & 0 \\ 0 & \underline{\tau}^{i+1}(\vec{k}^+(\vec{0})) \end{pmatrix} \begin{pmatrix} R^i(\vec{g}^+)\underline{1} & 0 \\ 0 & R^{i+1}(\vec{g}^+)\underline{1} \end{pmatrix} \tag{31}$$

and

$$\begin{pmatrix} \underline{T}^{i,i}(\vec{k}^-(\vec{g})) & \underline{T}^{i,i+1}(\vec{k}^-(\vec{g})) \\ \underline{T}^{i+1,i}(\vec{k}^-(\vec{g})) & \underline{T}^{i+1,i+1}(\vec{k}^-(\vec{g})) \end{pmatrix} = \begin{pmatrix} R^i(\vec{g}^-)\underline{1} & 0 \\ 0 & R^{i+1}(\vec{g}^-)\underline{1} \end{pmatrix} \begin{pmatrix} \underline{1} & -\underline{\tau}^i(\vec{k}^+(\vec{0}))\underline{\hat{G}}^{i,i+1}(\vec{k}^+(\vec{0})) \\ -\underline{\tau}^{i+1}(\vec{k}^+(\vec{0}))\underline{\hat{G}}^{i+1,i}(\vec{k}^+(\vec{0})) & \underline{1} \end{pmatrix}^{-1}$$
$$\times \begin{pmatrix} \underline{\tau}^i(\vec{k}^+(\vec{0})) & 0 \\ 0 & \underline{\tau}^{i+1}(\vec{k}^+(\vec{0})) \end{pmatrix} \begin{pmatrix} R^i(\vec{g}^-)\underline{1} & 0 \\ 0 & R^{i+1}(\vec{g}^-)\underline{1} \end{pmatrix}^{-1}. \tag{32}$$

The matrix inversions in Eqs. (31) and (32) involve the identical matrix independent of $\vec{g}$ and only *one* inversion is necessary. The next step is to form layer vectors ($i = 2$)

$$\overline{T}_{iL}(\vec{k}^\pm(\vec{g})) = \sum_{L'} [\overline{T}^{ii}_{LL'}(\vec{k}^\pm(\vec{g})) + \overline{T}^{ii+1}_{LL'}(\vec{k}^\pm(\vec{g}))] Y^*_{L'}(\vec{k}^\pm(\vec{g})) \tag{33}$$

and

$$\overline{T}_{i+1L}(\vec{k}^\pm(\vec{g})) = \sum_{L'} [\overline{T}^{i+1,i}_{LL'}(\vec{k}^\pm(\vec{g})) + \overline{T}^{i+1,i+1}_{LL'}(\vec{k}^\pm(\vec{g}))] Y^*_{L'}(\vec{k}^\pm(\vec{g})). \tag{34}$$

The matrices $\overline{T}^{ij}_{LL'}(\vec{k}^\pm(\vec{g}))$ and vector $\overline{T}_{iL}(\vec{k}^\pm(\vec{g}))$ for $i, j = 2, 3$ contains all multiple-scattering events that occur in layers 2 and 3. They form the elements of subgroup A. The difference between quantities $\overline{T}_{iL}(\vec{k}^\pm(\vec{g}))$ and $\overline{T}^{ij}_{LL'}(\vec{k}^\pm(\vec{g}))$ can be expressed in terms of the scattering paths that these quantities describe. $\overline{T}^{ij}_{LL'}(\vec{k}^\pm(\vec{g}))$ includes all scattering paths starting at layer j and terminating at layer i with any number (including zero) of intermediate scatterings off the layers. $\overline{T}_{iL}(\vec{k}^\pm(\vec{g}))$, on the other hand, includes all scattering paths that terminate at layer i, regardless of their origins.

The following step is to treat scattering events among layer 1, subgroup A and layer 4. The L-space iteration procedure given in Eqs. (5)–(7) must now be changed due to the fact that multiple scattering events between layers 2 and 3 have already been summed. The vectors $T_{iL}(\vec{k}^\pm(\vec{g}))$ are given by

$$T_{iL}(\vec{k}^\pm(\vec{g})) = \tau_{iL}(\vec{k}^\pm(\vec{g})) + \sum_{n=0}^{M} [T^-_{iL}{}^{(n)}(\vec{k}^\pm(\vec{g})) + T^+_{iL}{}^{(n)}(\vec{k}^\pm(\vec{g}))], \quad i = 1 \text{ or } 4 \tag{35}$$

and

$$T_{iL}(\vec{k}^\pm(\vec{g})) = \overline{T}_{iL}(\vec{k}^\pm(\vec{g})) + \sum_{n=0}^{M} [T^-_{iL}{}^{(n)}(\vec{k}^\pm(\vec{g})) + T^+_{iL}{}^{(n)}(\vec{k}^\pm(\vec{g}))], \quad i = 2 \text{ or } 3. \tag{36}$$

For layers 1 and 4, the new iteration relations for $T^{\mp(n)}_{iL}(\vec{k}^\pm(\vec{g}))$ are the same as before,

$$T^{\mp(n)}_{iL}(\vec{k}^\pm(\vec{g})) = \sum_{L_1L_2} \tau^i_{LL_1}(\vec{k}^+(\vec{0})) \sum_{\substack{j<i \\ j>i}} G^{ij}_{L_1L_2}(\vec{k}^\pm(\vec{g})) [T^{\mp(n)}_{jL_2}(\vec{k}^\pm(\vec{g})) + T^{\pm(n-1)}_{jL_2}(\vec{k}^\pm(\vec{g}))], \quad i = 1 \text{ or } 4. \tag{37}$$

For layers 2 and 3, $T^{\mp(n)}_{iL}(\vec{k}^\pm(\vec{g}))$ have the following different forms ($i = 2$):

$$T^{\mp(n)}_{iL}(\vec{k}^\pm(\vec{g})) = \sum_{L_1L_2} \sum_{\substack{j<i \\ j>i+1}} [\overline{T}^{ii}_{LL_1}(\vec{k}^\pm(\vec{g}))G^{ij}_{L_1L_2}(\vec{k}^\pm(\vec{g})) + \overline{T}^{ii+1}_{LL_1}(\vec{k}^\pm(\vec{g}))G^{i+1j}_{L_1L_2}(\vec{k}^\pm(\vec{g}))][T^{\mp(n)}_{jL_2}(\vec{k}^\pm(\vec{g})) + T^{\pm(n-1)}_{jL_2}(\vec{k}^\pm(\vec{g}))] \tag{38}$$

and

$$T^{\mp(n)}_{i+1L}(\vec{k}^\pm(\vec{g})) = \sum_{L_1L_2} \sum_{\substack{j<i \\ j>i+1}} [\overline{T}^{i+1,i}_{LL_1}(\vec{k}^\pm(\vec{g}))G^{ij}_{L_1L_2}(\vec{k}^\pm(\vec{g})) + \overline{T}^{i+1,i+1}_{LL_1}(\vec{k}^\pm(\vec{g}))G^{i+1j}_{L_1L_2}(\vec{k}^\pm(\vec{g}))][T^{\mp(n)}_{jL_2}(\vec{k}^\pm(\vec{g})) + T^{\pm(n-1)}_{jL_2}(\vec{k}^\pm(\vec{g}))]. \tag{39}$$

In Eqs. (37)–(39), the upper signs correspond to the upper sum over j (e.g., $j<i$) and vice versa. The initial conditions Eqs. (8) and (9) are unchanged, except for extension to general incident directions $\vec{k}^{\pm}(\vec{g})$

$$T_{1L}^{-(n)}(\vec{k}^{\pm}(\vec{g}))=0, \quad n=0,1,2,\ldots, \tag{40}$$

$$T_{N'L}^{+(n)}(\vec{k}^{\pm}(\vec{g}))=0, \quad n=0,1,2,\ldots; \quad N'=4. \tag{41}$$

The new starting conditions are

$$T_{4L}^{-(-1)}(\vec{k}^{\pm}(\vec{g}))=\tau_{4L}(\vec{k}^{+}(\vec{0})), \tag{42}$$

$$T_{1L}^{+(-1)}(\vec{k}^{\pm}(\vec{g}))=\bar{\tau}_{1L}(\vec{k}^{\pm}(\vec{0})), \tag{43}$$

and

$$T_{iL}^{-(-1)}(\vec{k}^{\pm}(\vec{g}))=T_{iL}^{+(-1)}(\vec{k}^{\pm}(\vec{g})) = \bar{T}_{iL}(\vec{k}^{\pm}(\vec{g})), \quad i=2 \text{ or } 3. \tag{44}$$

After convergence in the L-space iterations [Eqs. (37)–(39)] is reached, the layer vectors $T_{iL}(\vec{k}^{\pm}(\vec{g}))$ given in Eqs. (35) and (36) are used to form K-space transmission and reflection matrices $M_{\vec{g},\vec{g}}^{\pm\pm}$ for the 4-layer complex [see Eqs. (20)–(23)]. Scattering between the complex (layers 1–4) and deeper layers 5–N are solved in K space, since the remaining interlayer separations are assumed to be large.

VI. TEST CASE: CHEMISORPTION OF H ON Ni(001)

We have programmed this method to include the features mentioned. The summations involved in calculating $G_{LL'}^{ij}(\vec{k}^{\pm}(\vec{g}))$ are done in two ways, either in $\vec{g}$ space or $\vec{r}$ space, depending on the relative computation speed. Also, the program is designed such that L-space iteration, matrix inversion, or a combination of both may be chosen to treat groups of closely spaced layers, depending on the material and crystal structure. Symmetries are exploited in K space, considerably reducing the size of $M_{\vec{g},\vec{g}}^{\pm\pm}$ and thereby the computational effort required in producing these matrices. Since a structure search involves calculations done for a series of geometries, the program is designed to save time-consuming quantities that are not altered in a geometry change [e.g., many of the matrices $G_{LL'}^{ij}(\vec{k}^{\pm}(\vec{g}))$ may not be affected by a structure change and therefore need not be recomputed]. As a test case, the combined space method is applied to the situation of a 1×1 monolayer of hydrogen atoms on the (001) face of nickel. We allow the hydrogen monolayer and top nickel substrate layer are first treated by L-space iterations. Then transmission and reflection matrices for the double layer complex are found according to Eqs. (20)–(23). Scattering among deeper nickel layers and the double layer complex are treated by the RFS method. Reflected intensities for the (00), (11), and (20) beams for various hydrogen overlayer-nickel substrate separations are shown in Figs. 3–5. Phase shifts for hydrogen are obtained from a Hartree-Fock potential. The dynamical inputs (electron damping, vibration amplitudes, inner potential, phase shifts) for nickel are taken from those used in previous calculations of clean Ni(001).[21,22] We found that even at the smallest interlayer spacing, the L-space iterations converge rapidly and satisfactorily, and there is no need for matrix inversion in this case. This is probably due to the rather weak scattering of the hydrogen overlayer. Our test case cannot be compared to experiment, as no experimental data now exist for this system. However, it does serve as a valuable illustration of the ability of the combined space method in handling layers with very

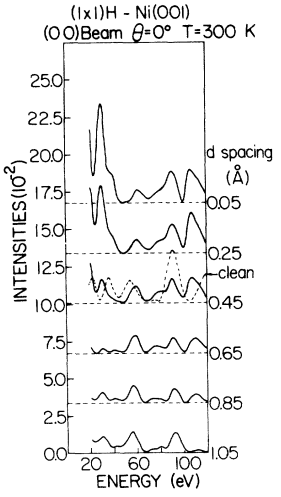

FIG. 3. (1×1)H-Ni(001) calculated intensity-voltage (I-V) curves for different d spacings between the H monolayer and the top nickel layer. The (00) beam is shown. The curve in broken line is the corresponding beam for clean Ni(001). The vertical scale of the clean Ni(001) curve is arbitrary. The hydrogen atom sits in a four-fold (hollow) site.

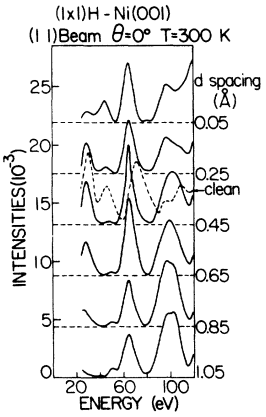

FIG. 4. Same as in Fig. 3, the (11) beam is shown.

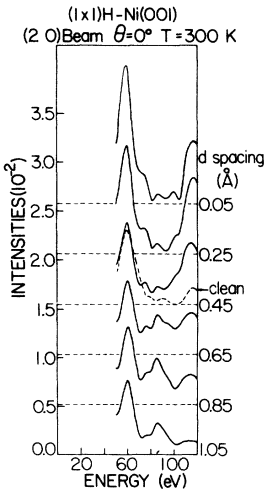

FIG. 5. Same as in Fig. 3, the (20) beam is shown.

small separation distances. A further test calculation was made in which a monolayer of Ni(111) was divided into four coplanar sublayers of 2×2 periodicity.[20] L-space iterations were carried out, as well as matrix inversion on two sublayers combined with layer iterations, and matrix inversion on all four sublayers. Results of the three procedures converge well to each other.

VII. CONCLUSION

We have presented the formulation of a unified method for the evaluation of reflected low-energy electron diffraction intensities based on an efficient coupling of L-space and K-space representations. The method is particularly useful in structural systems such as the reconstructed surfaces of transition metals, hydrogen or other gas atom chemisorption forming coplanar or near coplanar adsorbate layers, reconstructed or unreconstructed surfaces of semiconductors,[23] layer compounds,[24,25] etc., where groups of closely spaced layers are joined to other layers with larger separations. In the discussion in Sec. V, we picked an example having one group of closely spaced layers only. However, a lattice structure with various groups of closely spaced layers joined mutually or to other layers with larger interlayer spacings may similarly be treated.

We wish to point out that in combining scattering contributions from coplanar or near coplanar layers by Eqs. (20)–(23), the dimension of the matrices and vectors used is L. This is different from the conventional treatment of many atoms per unit cell in K-space methods, e.g., layer KKR, RFS, or layer doubling. In the K-space methods, multiple scatterings among different atoms in a unit cell of a layer are summed by inverting a matrix of form $(1-x)^{-1}_{LK,L'K'}$. The dimension of this matrix is $L\times K$, where K is the number of atoms in the unit cell. For the same coplanar or near coplanar lattice structure, for formulation given here is faster.

APPENDIX

To obtain Eq. (1), one requires that the beams that are to be included in the calculation are all those that decay by at most a factor t from one layer to the next. In the plane-wave representation, the propagation perpendicular to the surface through an interlayer distance d involves decay. These beams must satisfy the condition $|\exp[i\vec{k}^{\pm}(\vec{g})\cdot\vec{d}]|>t$, where $\vec{k}^{\pm}(\vec{g})$ is the complex wave vector of each beam. This condition will of course be satisfied by all "propagating beams," for which $|\vec{k}^{\pm}_{\parallel}(\vec{g})|^2 \le 2E$ (a.u.). For evanescent beams, $\vec{k}^{\pm}_{\perp}(\vec{g})$ has a large imaginary part, with an absolute value of $[|\vec{k}^{\pm}_{\parallel}(\vec{g})|^2-2E]^{1/2}$. Our criterion for inclusion becomes $[|\vec{k}^{\pm}_{\parallel}(\vec{g})|^2-2E]^{1/2}<(\ln t)/d$. This condition defines a circle in $\vec{k}_{\parallel}$ space and we wish to find the number g of reciprocal-lattice points included inside this circle. The number is given by the ratio of the area of the circle to the area of the unit cell in reciprocal space. The radius of the circle is obtained by replacing the inequality by the corresponding equality, yielding for the radius squared $|\vec{k}^{\pm}_{\parallel}(\vec{g})|^2=2E+[(\ln t)/d]^2$. If A is the unit cell area in direct space, then the unit cell area in reciprocal space is $(2\pi)^2/A$. So the required ratio, i.e., the number of beams to be included, becomes

$$g=\frac{|\vec{k}^{\pm}_{\parallel}(\vec{g})|^2}{(2\pi)^2/A}=\frac{A}{4\pi}\left[2E+\left(\frac{\ln t}{d}\right)^2\right],$$

which is Eq. (1)

*Work supported in part by NSF Grant No. DMR73-02614 and by the Graduate School Research Committee, University of Wisconsin-Milwaukee.

†Present address: Department of Chemical Engineering, California Institute of Technology, Pasadena, Calif.

[1]See, for example, S. Y. Tong, in *Progress in Surface Science*, edited by S. G. Davisson (Pergamon, New York, 1975), Vol. 7, No.1.

[2]N. Stoner, M. A. Van Hove, and S. Y. Tong, in *Advances in the Characterization of Metal and Polymer Surfaces*, edited by L. H. Lee (Academic, New York, 1976).

[3]J. L. Beeby, J. Phys. C 1, 82 (1968).

[4]E. G. McRae, Surf. Sci. 11, 479 (1968).

[5]P. J. Jennings and E. G. McRae, Surf. Sci. 23, 63

(1970).
[6]D. W. Jepsen, P. M. Marcus, and F. Jona, Phys. Rev. Lett. 26, 1365 (1971).
[7]D. W. Jepsen, P. M. Marcus, and F. Jona, Phys. Rev. B 5, 3933 (1972).
[8]J. A. Strozier, Jr. and R. O. Jones, Phys. Rev. Lett. 25, 516 (1970).
[9]S. Y. Tong and T. N. Rhodin, Phys. Rev. Lett. 26, 711 (1971).
[10]R. H. Tait, S. Y. Tong, and T. N. Rhodin, Phys. Rev. Lett. 28, 553 (1972).
[11]P. J. Jennings, Surf. Sci. 41, 67 (1974).
[12]J. B. Pendry, Phys. Rev. Lett. 27, 856 (1971).
[13]S. Y. Tong, Solid State Commun. 16, 91 (1975).
[14]J. B. Pendry, *Low-Energy Electron Diffraction Theory* (Academic, London, 1974).
[15]M. A. Van Hove and J. B. Pendry, J. Phys. C 8, 1362 (1975).
[16]M. A. Van Hove and S. Y. Tong, J. Vac. Sci. Technol. 12, 230 (1975).
[17]M. A. Van Hove and S. Y. Tong, Phys. Rev. Lett. 35, 1092 (1975).
[18]M. A. Van Hove and S. Y. Tong, Surf. Sci. 54, 91 (1976).
[19]See, for example, T. N. Rhodin and S. Y. Tong, Phys. Today 28, 23 (1975).
[20]R. S. Zimmer and B. W. Holland, J. Phys. C 8, 2395 (1975).
[21]S. Y. Tong and L. L. Kesmodel, Phys. Rev. B 8, 3753 (1973).
[22]J. E. Demuth, P. M. Marcus, and D. W. Jepsen, Phys. Rev. B 11, 1460 (1975).
[23]A. R. Lubinsky, C. B. Duke, B. W. Lee, and P. Mark, Phys. Rev. Lett. 36, 1058 (1976).
[24]B. J. Mrstik, S. Y. Tong, R. Kaplan, and A. K. Ganguly, Solid State Commun. 17, 755 (1975).
[25]B. J. Mrstik, R. Kaplan, T. L. Reinecke, M. A. Van Hove, and S. Y. Tong, Phys. Rev. B 15, 897 (1977).